CHAPTER II

THEORETICAL BACKGROUND AND LITERATURE REVIEW

2.1 Membrane for Gas Separation

A membrane, by definition, is a barrier film which allows selective and specific permeation under conditions appropriate to its function (Vieth, 1991). A membrane separation system separates an influent stream into two effluent streams which are permeate and concentrate. The permeate is the stream that passes through the semi-permeable membrane whereas the concentrate is the portion of the influent stream that has been retained by the membrane.

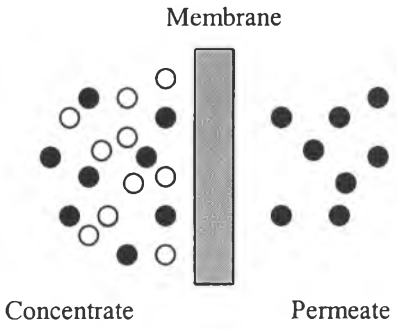

Figure 2.1 Membrane separation process.

Diverse types of membranes have been developed depending on the objective of the application: microfiltration, ultrafiltration, nanofiltration, reverse osmosis, gas separation, pervaporation etc. The morphologies of membranes play an important role in the production of membranes. They can be categorized into two classes as shown in Fig.2.3: symmetric and asymmetric membranes (Mulder, 1991). Symmetric membranes are prepared by solution casting or thermal melt processing processes while asymmetric membranes are made up of a thin dense skin with a porous support layer underneath. Separation is generally performed on the top surface layer of the membranes.

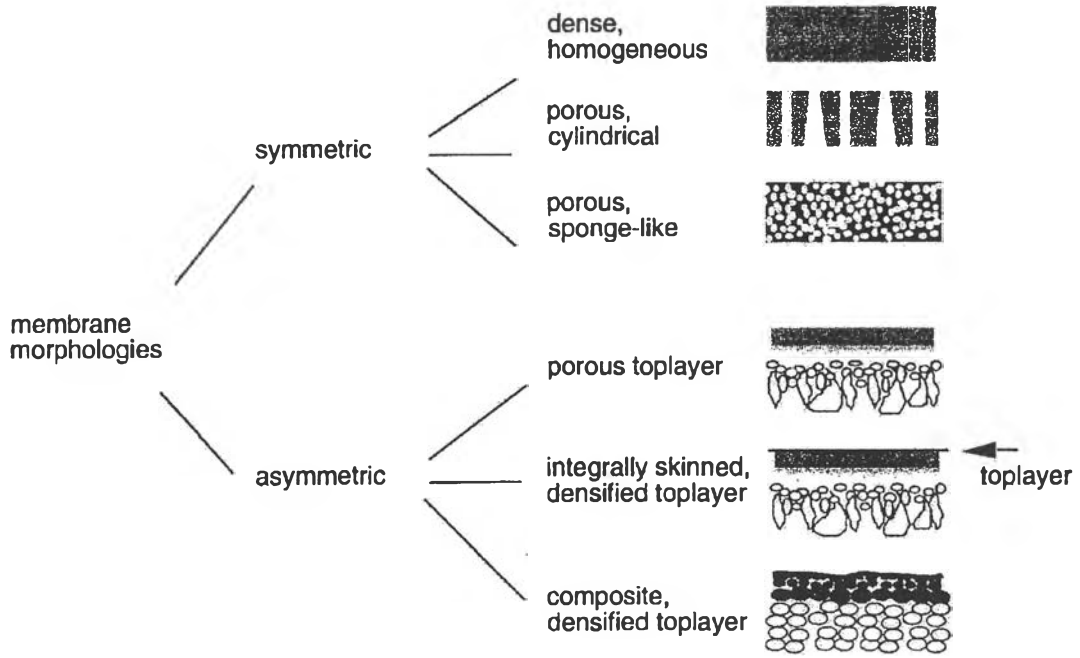

Figure 2.2 Schematic representation of different membrane morphologies (Mulder, 1991).

The first class, the symmetric membranes, can be divided into three groups of membranes:

- Homogeneous, dense membranes with an active layer thickness of more than 10 μm;
- Cylindrical porous membranes;
- Sponge-like porous membranes; these membranes usually have an average pore size of 0.2-5 μm.

The second class, the asymmetric membranes, can be also subdivided into three groups:

- Porous membrane; here, the membrane does not have the same pore size over the whole membrane thickness but a pore size gradient;
- Porous membranes having a top layer (integrally-skinned membranes); these membranes normally have a second layer with much smaller pores

(5-500 μm) atop an open, porous support layer. Alternatively, the top layer may be dense that only gas can penetrate through the film;

- Composite membranes; a homogeneous layer is placed in a second production step on top of a support membrane.

Applications of membranes in gas separation are in a wide variety of areas, such as hydrogen recovery, carbon dioxide removal, oxygen and nitrogen separation, helium recovery from natural gas, and dehydration of air. Asymmetric-type membranes are satisfactory for gas separation processes since they provide more transmembrane flux for commercial separation processes than the symmetric membranes. There are three types of membranes used in gas separation membranes, namely Knudsen diffusion membranes, Molecular sieving membranes and Solution-diffusion type membrane.

2.1.1 Knudsen Diffusion Membranes

In a Knudsen diffusion membrane, gas transport is dominated by the Knudsen flow separation mechanism.

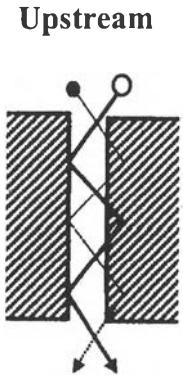

Figure 2.3 Mechanism of Knudsen flow of gas molecules.

The mechanism depends upon the pore size of the membrane (r), and the mean free-path of the gas molecules (λ). When $r < \lambda$, the majority of the collisions are between the gas molecules and the pore wall, resulting in faster transport of the lighter gas molecules than the heavier ones.

The selectivity (α_i) of this kind of separation can be obtained on the basis of the inverse square root ratio of the molecular mass (M_i) of the diffusing species, i.

$$\alpha_{A/B} = \sqrt{\frac{M_B}{M_A}} \tag{1}$$

Membranes which have a pore size less than 0.5 μm are classified as Knudsen diffusion membranes. Normally, those membranes are made of oxides (Alumina, Zirconia, Titania), ceramic and glass. They do not provide a high degree of separation due to their large pore sizes, but they do provide stability at high temperature and also corrosion resistance. Therefore, new technologies to make more selective membranes as well as development of the applications of Knudsen diffusion membranes are still growing today.

One of the most recent technologies to fabricate Knudsen diffusion membranes has been proposed by Kinemuchi and co-workers in 2001. The process consists of two steps: ultrafme powder production and membrane deposition. Figure 2.4 illustrates the experimental setup of the process.

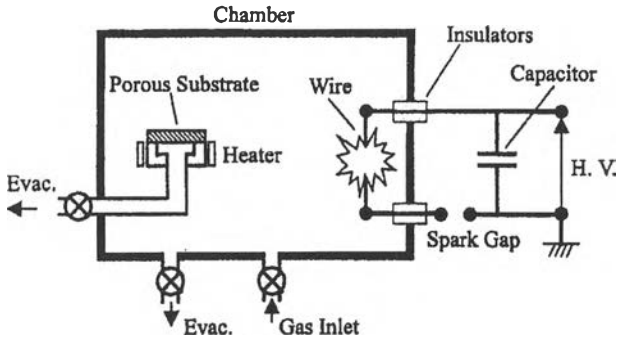

Figure 2.4 Schematic illustration of the experimental setup (Kinemuchi *et al.*, 2001).

First, the aluminum plasma is generated by passing high current through an aluminum wire in an oxygen atmosphere. The aluminum plasma cools uniformly and rapidly in the oxygen gas producing an aerosol of ultrafme aluminum oxide powder. The powder then deposits on a porous alumina substrate which is kept at

500, 600 or 700°C for 30 minutes. The powder is sintered during deposition, resulting in a ceramic layer with very fine pores on top of the substrate. Figure 2.5 shows SEM photographs of the filter surfaces before and after powder deposition with different substrate temperatures. The separation of H_2/CH_4 and H_2/O_2 has been conducted using powder-deposited membranes obtained with different sintering temperatures to determine the performance of the membranes.

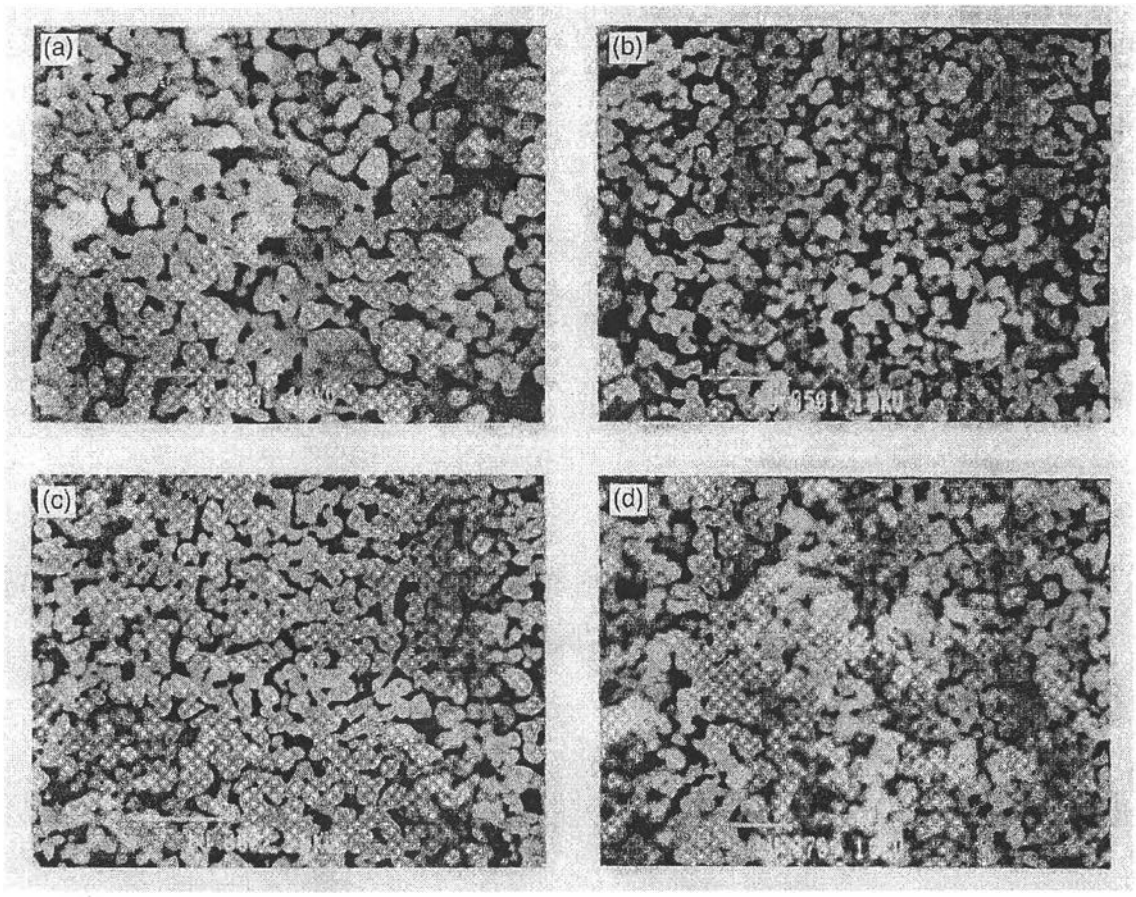

Figure 2.5 SEM photographs of surfaces of (a) substrate and of filters deposited at (b) 500°, (c) 600°, and (d) 700° C (Kinemuchi *et al.*, 2001)

The results are shown in terms of the permselectivities for H_2/CH_4 and H_2/O_2 as functions of sintering temperatures along with the theoretical permselectivities of Knudsen diffusion (Fig. 2.6). According to the Knudsen diffusion principle, the permselectivities for H_2/CH_4 and H_2/O_2 are 4.0 and 2.8, respectively. As shown in Figure 2.6, the higher the substrate temperature, the higher the permselectivities, and the more they approach those of the Knudsen flow, which indicates that the pore

radius is smaller for membranes obtained at a higher substrate temperature. The deviation of the permselectivities decreases as the temperature increases relating to the uniformity of the pore structure.

Hence, a fine and uniform pore-sized membrane that can be used in hydrogen/oxygen or hydrogen/ methane separations can be produced at a sintering temperature of 600°C or higher.

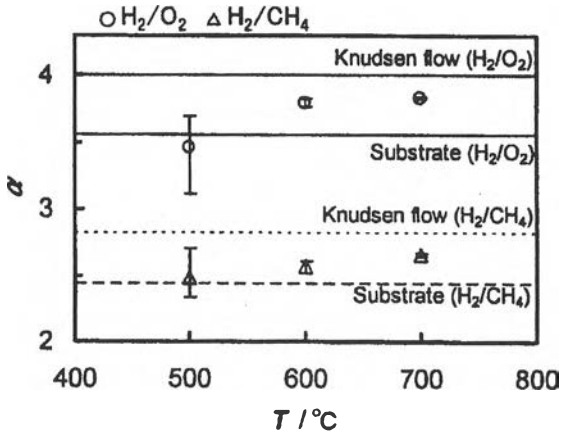

Figure 2.6 Permselectivity (α) for H_2/CH_4 and H_2/O_2, as a function of sintering temperature (T). (Note that the deviation at 500°C is of the same order as that of the substrate) (Kinemuchi *et al.*, 2001).

For application of a Knudsen diffusion membranes, a ZrO_2-SiO_2 porous membrane has been used in a reactor for hydrogen production from hydrogen sulfide (Ohashi *et al.*, 1998). Due to the problem caused by sulfur in the petroleum refinery, a hydrodesulfurization process has been developed to reduce the sulfur content of the crude oil before it is sent to the distillation unit. From this process, a by-product, hydrogen sulfide has been produced in a huge amount resulting in a waste of valuable hydrogen. To recover hydrogen, a process to decompose hydrogen sulfide has been established. The process is based on the chemical reaction shown below;

$$H_2S \leftrightarrow H_2 + 1/x\ S_x \qquad (2)$$

The reaction is highly endothermic and the equilibrium conversions are low. Hence, the decomposition of H_2S must be done at high temperature, usually above 1000 K and preferably at 1800 K. In addition, to gain a higher degree of conversion, one of the products of the reaction should be removed. Thus, a ZrO_2-SiO_2 composite membrane which shows Knudsen diffusion characteristic is introduced into the specially designed reactor to remove hydrogen. The design of the reactor is illustrated in Figure 2.7.

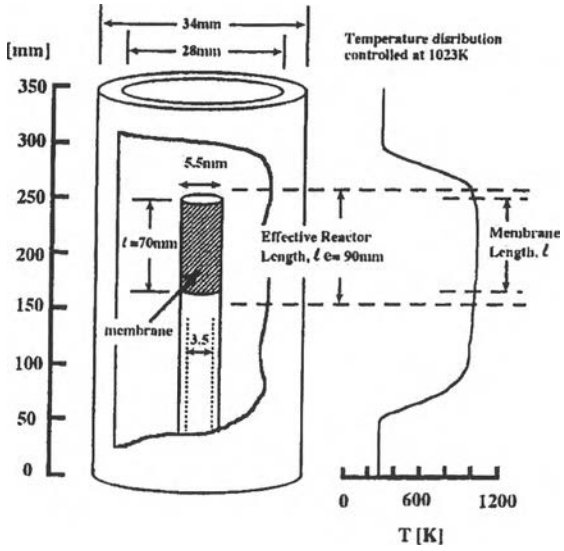

Figure 2.7 A cut view of the reactor cell for recovering hydrogen from hydrosulfurization process (Ohashi *et al.*, 1998).

With the temperature of 1023 K, reactor pressure of 0.11 Mpa absolute, pressure in the permeate chamber of 5 kPa and inlet flow rate of H_2S of 3.2×10^{-5} mol/s, the membrane integrated reactor gave the highest H_2 fraction in the permeate chamber of 0.22. This value is four times higher than the equilibrium value at the same condition without using the membrane.

2.1.2 Molecular Sieving Membranes

A membrane which separates a gas mixture by means of molecular sieving is normally an ultramicroporous-type membrane. The separation is based principally on the much higher diffusion rate of the smaller molecule. Materials that exhibit molecular sieving properties are inorganic such as silica, zeolites and carbon.

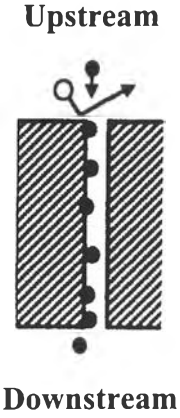

Figure 2.8 Mechanism of flow of gas molecules in molecular sieving membrane.

Among the materials that molecular sieving membranes can be made of, carbon is the most interesting one since it is more feasible to form a large, defect-free carbon membrane than zeolite or silica-based membrane. As well, the carbon membrane provides a smaller pore size than the other two kinds of membranes. The carbon membrane contains constrictions in the carbon matrix that approach the molecular dimensions of the diffusing species. In this manner, diffusing gas molecules can be discriminated based upon the size and the shape of the molecules. Even the slightly different sized gas molecules can be effectively separated, as the diffusing molecules are activated to pass through the constrictions that are sufficiently small relative to their size. Important applications of carbon membranes are in the production of low cost and high purity nitrogen from air, hydrogen separation from gasification gas and purification of methane. In addition, carbon membranes are reported to be among promising candidates for the separation of light alkenes/alkanes such as propene/propane.

Compared with an organic membrane, a polymeric dense membrane in which the separation is based on the solution-diffusion, the molecular sieving membranes provide higher selectivity and productivity. Molecular sieving membranes are suitable to be used in separation processes with high temperature in the range of 500-900°C whereas organic polymer membranes cannot resist very high temperature and tend to decompose or react with some chemical. However, high production cost, durability (the membrane is very brittle and fragile), fouling and difficulties in large-scale use are still some of the unsolved problems in the molecular sieving membranes. As a result, a lot of effort has been put into research concerning the economically practicable ways to produce high performance molecular sieving membranes.

Mixed-matrix composite membrane is one of the new technologies that has been developed recently for the improvement of molecular sieving membrane. The mixed-matrix membrane is comprised of molecular sieve material within a polymer substrate which offers the potential to combine the processability of polymers with the superior gas separation properties of rigid molecular sieving materials such as zeolite and silicalite. Figure 2.9 shows steps to construct a zeolite mixed-matrix membrane.

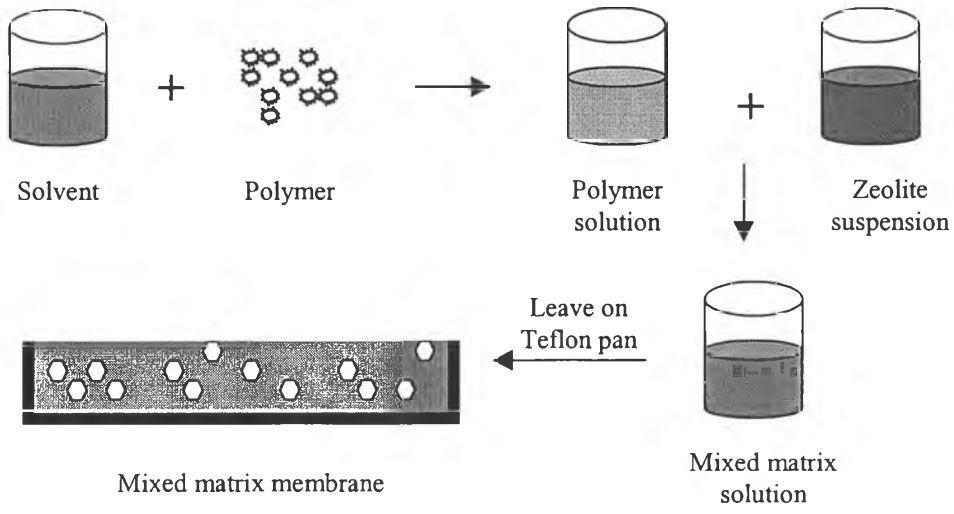

Figure 2.9 Fabrication of mixed matrix membrane.

It was reported that the addition of molecular sieve materials improved pure polymer selectivities (Kulprathipanja *et al.*, 1988, and Ismail and David, 2001).

2.1.3 Solution-diffusion Type Membranes

The solution-diffusion type membranes are non-porous polymeric membranes. They do not separate species on the basis of an ordinary sieving mechanism (depicted in Figure 2.10). The mechanism for dense polymeric membranes is the so-called solution-diffusion mechanism, which involves diffusivity and solubility of the gas molecules in membrane material. Diffusivity selectivity favors the smallest molecule whereas solubility selectivity favors the most condensable one.

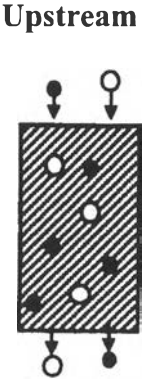

Figure 2.10 Solution-diffusion transport mechanism.

The state of the polymer, rubbery or glassy, is a factor involved in the transport of gas molecules inside the polymer material.

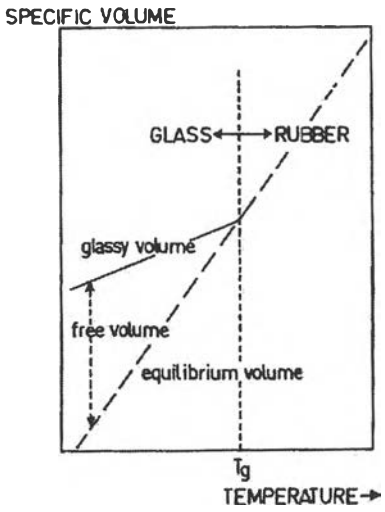

Figure 2.11 Glass transition of polymers (Bitter, 1991).

The glass transition temperature (T_g) is a distinction between the two states of polymers. Polymers above the T_g are defined as rubbery polymers while below the T_g they are defined as glassy polymers. In glassy state, the thermal volumetric expansion coefficient of a polymer is smaller than in the rubbery state (see Figure 2.11). This is attributed to the extraordinarily long relaxation time for polymer chains below the T_g, resulting in a nonequilibrium excess volume in glassy polymers.

Commercial membranes used for the separation of supercritical gases (i.e. those gases whose critical temperature is above ambient) such as air separation, H_2 recovery from ammonia purge gas, and CO_2 removal from natural gas are glassy polymers. Because of the more restricted mobility of the polymer structure, glassy polymers exhibit higher diffusivity selectivity than rubbery polymers. As mentioned, Figure 2.12 illustrates the diffusion coefficients of the penetrants as a function of critical volume, a commonly used indicator for penetrant size, in *cis*-polyisoprene, a rubbery polymer, and poly(vinyl chloride) (PVC), a glassy polymer. It can be seen that diffusion coefficients are higher in rubbery polyisoprene, however, the effect of penetrant size on diffusivity is much greater for glassy PVC. So it is clear that glassy polymers are more useful as membranes for supercritical gas separation than rubbery polymers.

In contrast to the point mentioned above, polymer membranes that exhibit high diffusivity selectivity are not suitable for the separation of large, condensable organic vapors from supercritical gases. For the separation of volatile organic compounds, VOCs, from process effluent air streams, and the removal of higher hydrocabons such as propane and butane from raw natural gas, the large gas molecules are typically the minor components. Therefore, membranes in these applications are required to be more permeable to large molecules to minimize membrane area and compression requirements.

Figure 2.13 depicts the permeability of glassy polysulfone (PSF) and rubbery *cis*-polyisoprene to a series of penetrants as a function of critical volume, which is, again, used as a measure of penetrant size. From the figure, the rubbery polymer membrane exhibits much higher permeabilities to the large molecules than the glassy polymer. As a result, polymers such as cis-polyisoprene and rubbery polydimethylsiloxane (PDMS) are required for these applications (Freeman and Pinnau, 1997).

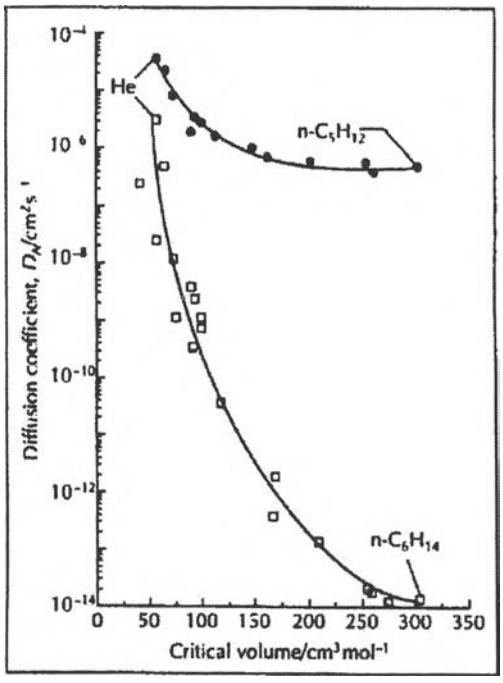

Figure 2.12 Effect of penetrant size on diffusion coefficients in a rubbery polymer (•, *cis*-polyisoprine; T=50°C0) and a glassy polymer (□, poly(vinyl chloride); T=30°C (Freeman and Pinnau, 1997).

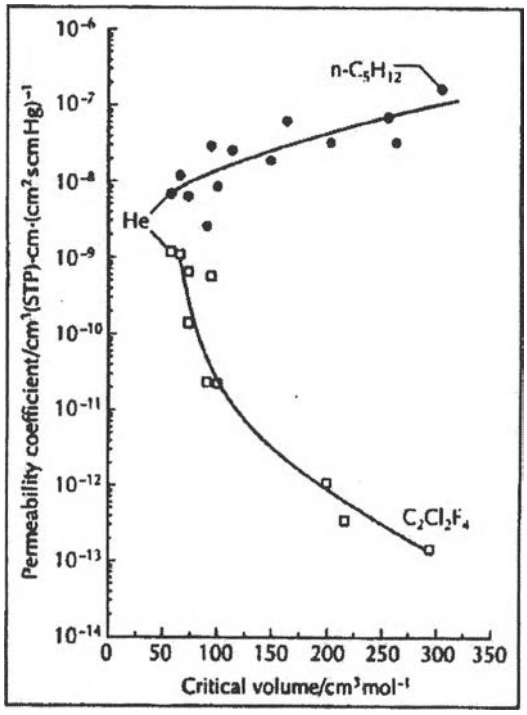

Figure 2.13 Effect of penetrant size on permeability coefficients in rubbery *cis*-polyisoprine (•) and low-free-volume, glassy polysulfone (□) (Freeman and Pinnau, 1997).

2.2 Transport of Gas Through Polymeric Dense Membrane

2.2.1 Solution-diffusion Mechanism

Gas separation with a polymeric dense membrane takes place according to a solution-diffusion based mechanism. Penetrant transport through the membrane depends on the property of the material to be penetrated and traversed by the gas molecules (Kesting and Fritzsche, 1993). The mechanism consists of five consecutive stages (Crank and Park, 1968) and they are depicted in Fig 2.14.

1) Diffusion through the limit layer of the side corresponding to the higher partial pressure (upstream side);
2) Absorption of the gas (by chemical affinity or by solubility) by the polymer;
3) Activated diffusion of the gas inside the membrane polymer;

4) Desorption of the gas at downstream side;

5) Diffusion through the limit layer of the downstream side.

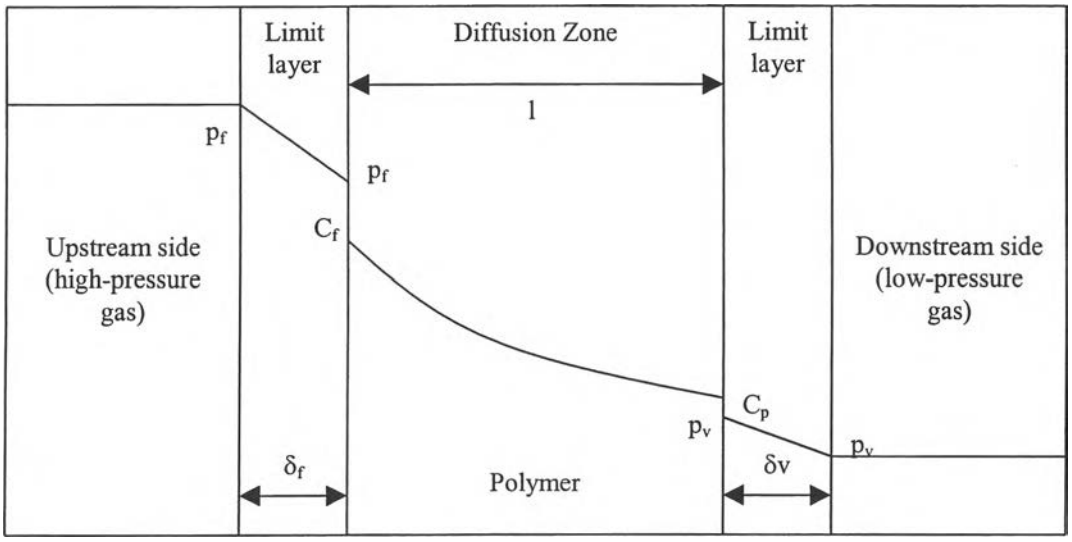

Figure 2.14 Schematic representation of the different resistances encountered by a molecule diffusing through a dense polymer membrane at a fixed temperature.

However, the resistances associated with stage 1) and stage 5) are normally negligible relative to the others so the transport of a gas molecule through a polymeric dense membrane is normally considered to consist of three steps; step 2), 3) and 4) (Kesting and Fritzsche, 1993).

2.2.2 Gas Transport Parameters

The gas transport in a non-porous membrane is governed by Fick's first law of diffusion, which states that the flux J is proportional to the concentration gradient ($\partial c/\partial x$) as:

$$J = -D\left(\frac{dc}{dx}\right) \tag{3}$$

Here, D is the diffusion coefficient. Eq (3) is applicable in the steady state, when the diffusion does not vary with time, and the flux is constant and occurs only in one

direction (x). On the other hand, Fick's second law (Eq. 4) describes the unsteady state of transport process.

$$\frac{dc}{dt} = D\left(\frac{dc^2}{d^2x}\right) \tag{4}$$

In the steady state, Eq. (3) may be integrated to give

$$J = D\frac{(c_1 - c_2)}{l} \tag{5}$$

where c_1 and c_2 are the concentrations of penetrant at the feed and permeate sides, respectively and l is the thickness of the membrane.

Henry's law (Eq 5) relates the concentration, c_i, of gaseous component i at the surface of the polymeric membrane to the partial pressure, p_i, of this component in the vapor phase in contact with it:

$$c = Sp \tag{6}$$

where S is the solubility coefficient. A combination of Eq. (5) and (6) gives

$$J = DS\frac{p_1 - p_2}{l} \tag{7}$$

where p_1 and p_2 are the pressure on the two sides of the membrane. The product of the diffusion coefficient and the solubility coefficient is now defined as the permeability coefficient, P:

$$P = DS \tag{8}$$

So in terms of permeability, the flux in Eq. (7) can be written as

$$J = P\frac{(p_1 - p_2)}{l} \tag{9}$$

2.2.3 Effect of Temperature on The Transport Parameters

A great number of data in literature suggests that the transport coefficients (P, D and S) depend on temperature, at a given pressure and a range of temperature, described by Arrhenius's law.

$$P = P_0\left(e^{-E_P/RT}\right) \tag{10}$$

$$D = D_0\left(e^{-E_D/RT}\right) \tag{11}$$

$$S = S_0\left(e^{-\Delta H_S/RT}\right) \tag{12}$$

where E_P and E_D are the activation energies of diffusion and permeation, respectively. ΔH_S is the heat of solution of the penetrant in the polymer and P_0, D_0 and S_0 are the pre-exponential factors. From the relationship of P, D and S, then, E_P, E_D and ΔH_S are linked as follows:

$$E_P = E_D + \Delta H_S \tag{13}$$

These parameters depend on the morphology and state of the polymer. The heat of solution, ΔH_S, the sum of the molar heat of condensation (ΔH_{cond}) and the partial molar heat of mixing (ΔH_l):

$$\Delta H_S = \Delta H_{cond} + \Delta H_l \tag{14}$$

The molar heat of condensation (ΔH_{cond}) is always negative. For supercritical gases (e.g. H_2, N_2, O_2 at room temperature), ΔH_{cond} is very small. On the other hand, the partial molar heat of mixing is a small and positive term, which can be estimated

from the cohesive energy densities of the penetrant and the polymer by using Hilderbrand's theory:

$$\Delta H_l = V_1(\delta_1-\delta_2)^2 \phi_2^2 \qquad (15)$$

δ_1 and δ_2 are the square roots of the cohesive energy densities of the penetrant and the polymer, which are parameters of solubility. V_1 is the partial molar volume of the penetrant and ϕ_2 is the volume fraction of the polymer in the mixture.

For the transport of supercritical gases, i.e. when ΔH_{cond} is very small, the heat of solution (ΔH_S) is then governed by ΔH_l alone. As a result, solubility (S) will increase with temperature. In the case of more condensable gases (e.g. CO_2, SO_2, NH_3 and hydrocarbons), ΔH_{cond} is strongly negative so the solubility decreases with increasing temperature. This illustrates that it is more difficult for these more condensable gas molecules to condense in the polymer when the temperature is higher.

The activation energy of diffusion (E_D) is the energy that a molecule requires to overcome the attractive forces between chains and create a hole in the polymer structure for the molecule to penetrate in.

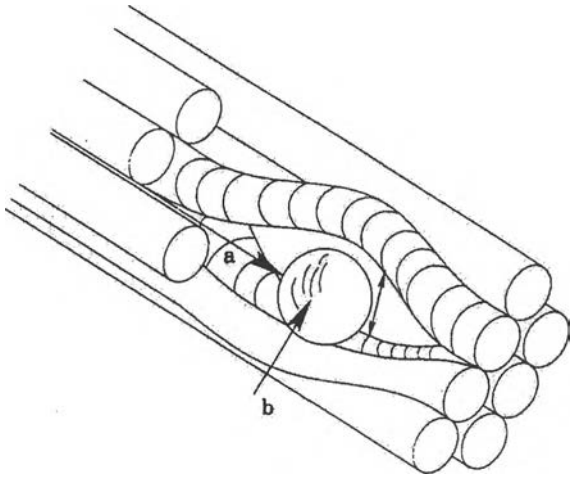

Figure 2.15 Molecular transport of penetrant through polymer chains where *a* indicates motion along parallel chains and *b* indicates the process of jumping into an adjacent tube (Vieth, 1991).

E_D is always positive so diffusivity (D) will increase with increasing temperature. In addition, when the size of the diffusing molecule is concerned, the diffusivity always increases as the penetrant size increases because the bigger molecule requires more activation energy to create bigger space to diffuse in the polymer matrix. Moreover, it is important to note that E_D of the rubbery polymer is found to be greater than that of the glassy polymer (George and Thomas, 2001 and Klopffer and Flaconneche, 2001).

2.2.4 Transport by Laminate

In a composite membrane, the transport of gas molecules will take place at different rates in each membrane layer, depending upon the gas transport properties of that layer.

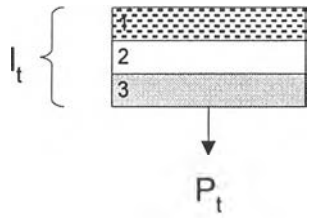

Figure 2.16 A three-layer composite membrane.

The permeability of each layer will contribute to the permeability of the composite membrane, as described in Eq. (16) (Tuwiner, 1962).

$$\frac{l_t}{P_t} = \frac{l_1}{P_1} + \frac{l_2}{P_2} \ldots + \frac{l_n}{P_n} \tag{16}$$

where P_t and l_t are Permeability and thickness of the composite,

P_1 and l_1 are Permeability and thickness of layer 1,

P_2 and l_2 are Permeability and thickness of layer 2,

P_n and l_n are Permeability and thickness of layer n,

The great majority of laminates or barriers in series appears to relate well with this equation. However, the equation can not be applied to a laminate that is dependent on pressure.

2.2.5 Transport of Mixed Gas

The most important parameter in the mixed gas transport is the selectivity of the membrane, also called the permselectivity. For a binary system, the permselectivity is defined as

$$\alpha_{A/B} = \frac{y_A / y_B}{x_A / x_B} \tag{16}$$

where y_i is the mole fraction of component i in the gas mixture at the permeate side and x_i is the mole fraction of component i at the feed side of the membrane. Assuming that the second gas does not have any effect on the solubility and diffusivity of the other gas, the selectivity of the membrane is then calculated by the ratio of the pure gas permeability of the two components through the membrane, determined under the same conditions. The selectivity parameter implies the separation property of the membrane in the sense of which gas the membrane prefers to let pass through. When $\alpha_{A/B} > 1$, it means that the transport of gas A through that given membrane is better than that of gas B so gas A is expected to be the majority of the gaseous phase in the downstream side of the membrane and vice versa.

$$\alpha_{A/B} = \frac{P_A}{P_B} = \left(\frac{D_A}{D_B}\right)\left(\frac{S_A}{S_B}\right) \tag{17}$$

The term shown in Eq. (18) is defined as the ideal selectivity of the mixed gas system. Both the diffusivity and the solubility are taken into account in the selectivity, which assists in assessing the selective nature of the membrane in terms of its thermodynamic (S) and kinetic (D). However, the selectivity calculated by Eq.

(18) can lead to an erroneous selectivity value since the mass transport in the mixed gas system is more complex than in the pure gas. In the case of a mixed gas system, the presence of one gas may affect the transport of the other due to a coupling effect. The interactions between mixed gases, or the interactions between gases and the polymer can change the gas permeability and membrane selectivity.

Dhingra and Marand (1998) determined gas transport parameters in pure and mixed CO_2 and CH_4 systems in two kinds of polymers which were a rubbery Poly (dimethyl siloxane); PDMS, membrane and a glassy Polyimide; NEW-TPI, membrane. The compositions for the mixed gas experiments were 5%, 25%, 50%, and 75% CO_2.

The values of the transport parameters over the feed gas concentrations are shown in Figure 2.17 for the rubbery membrane and 2.18 for the glassy membrane. It is obviously seen that the diffusion coefficient of the gas as a mixture in PDMS membrane does not change. Moreover, the permeability coefficient increases with CO_2 feed concentration, which is believed to be due to the increase in the solubility of the gas mixture. For NEW-TPI membrane, the higher the CO_2 feed concentration, the higher the values of diffusion and solubility coefficients of the gas mixture.

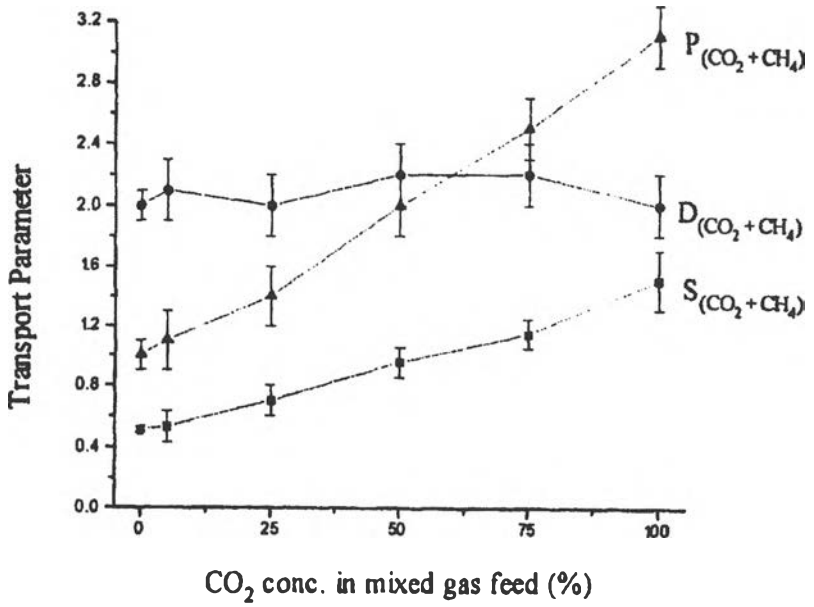

Figure 2.17 Change in overall transport parameter values with mixed gas feed concentration for PDMS membrane (**Note**: the units for P, D, and S are 10^{-1} Berrer; 10^{-9} cm^2/s; 10^{-2} cc(STP)/cc-cmHg; respectively) (Dhingra and Marand, 1998).

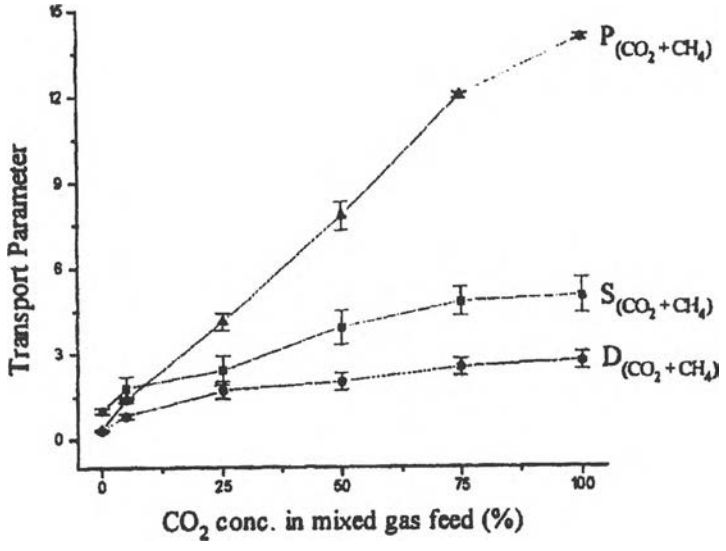

Figure 2.18 Change in overall transport parameter values with mixed gas feed concentration for NEW-TPI membrane (**Note**: the units for P, D, and S are 10^{-1} Berrer; 10^{-9} cm^2/s; 10^{-2} cc(STP)/cc-cmHg; respectively) (Dhingra and Marand, 1998).

Table 2.1 Value of solubility, diffusion and permeability coefficients of mixed gas and pure gas permeation in PDMS membrane at 35°C and 150 cmHg total feed pressure.

Feed	CO_2			CH_4		
	S	D	P	S	D	P
Mixed gas, 75% CO_2	1.3	2.4	3.1	0.37	2.4	0.89
Mixed gas, 50% CO_2	1.4	2.3	3.2	0.42	2.1	0.88
Mixed gas, 25% CO_2	1.5	2.0	3.0	0.47	2.0	0.94
Mixed gas, 5% CO_2	1.3	2.0	2.6	0.47	2.1	0.99
Pure gas	1.5	2.0	3.0	0.50	2.0	1.0
Maximum error	0.1	0.2	0.3	0.03	0.1	0.05

Table 2.2 Value of solubility, diffusion and permeability coefficients of mixed gas and pure gas permeation in NEW-TPI membrane at 35°C and 150 cmHg total feed pressure.

Feed	CO_2			CH_4		
	S	D	P	S	D	P
Mixed gas, 75% CO_2	10.1	1.6	16.2	0.13	1.8	0.23
Mixed gas, 50% CO_2	10.7	1.5	16.1	0.13	2.0	0.26
Mixed gas, 25% CO_2	10.0	1.7	17.0	0.13	2.0	0.26
Mixed gas, 5% CO_2	11.6	1.6	18.6	0.16	2.2	0.35
Pure gas	5.1	2.7	13.8	1.00	0.38	0.38
Maximum error	0.1	0.2	0.3	0.03	0.1	0.05

Note: the units for P: 10^3 Berrers;

D: 10^{-5} cm^2/s;

S: 10^{-2} cc(STP)/cc-cmHg.

Tables 2.1 and 2.2 show the transport parameter values of mixed gas and pure gas permeation in the rubbery and the glassy membranes, respectively. For the pure gas permeation, CO_2 solubilities are higher than those of CH_4 in both PDMS and NEW-TPI membranes. The diffusivities of both CO_2 and CH_4 in PDMS were the same while, in the glassy polymer, the diffusivity of CO_2 was higher than that of CH_4. We can find no difference when comparing the pure gas transport parameter values between the pure gas and the mixed gas in rubbery PDMS membrane. In contrast, the transport properties in the glassy membrane change when there is a

presence of a second gas component. So it can be concluded that the coupling effect occurs only in glassy polymer membranes. The competitive sorption between CO_2 and CH_4 in the mixed gas system was observed when there is an increase in the solubility coefficient of CO_2 in the presence of CH_4. In the case of diffusivity, the presence of CO_2 causes CH_4 to diffuse faster through the polymer matrix. However, the solubility effect of CO_2 is dominant in this system so the membrane shows higher CO_2 permeability.

2.3 The Search for Cl_2-Resistant Materials

Chlorine is an extremely reactive gas. It rapidly degrades many materials that it comes in contact with. However, there are a number of materials reported to be stable when left in a chlorine atmosphere for a certain period of time. In literatures, the chlorine-stable materials are found to be used for three purposes, which are corrosion-resistance devices, membrane separation and protective coatings.

For the first purpose, Teflon® or polytetrafluorethylene (PTFE) is used worldwide to make parts, case or the body of devices while come in contact with chlorine. Moreover, Fluorodine® Caulk (made with fluoroelastomer or Viton®) and polyvinylchloride (PVC) are often used in tubing system in many processes involving chlorine.

In the case of membrane separation, membranes made from silicone rubber or polydimethylsiloxane (PDMS), and carbon are used in the separation of chlorine from a mixed gas stream. Silicone rubber (PDMS) membrane is a solution-diffusion type rubbery polymer membrane which favors chlorine. On the other hand, carbon membrane is a molecular sieve type, which separates gases based on their molecular sizes. Therefore, a well-tailored carbon molecular sieve (CMS) membrane, in theory, will retain chlorine perfectly and let other smaller gases pass through.

Lokhandwala and coworkers (1999) invented a membrane process to recover chlorine from Chlor-alkali plant tail gas using a spiral wound membrane module fabricated with PDMS membrane. The tail gas generally contains 20% of chlorine, 50-70% of air with the balance of hydrogen and carbon dioxide. The result of the

field test showed that the membrane module was stable for about one month of continuous operation.

Performance in chlorine separation of four different membrane types was studied by Hagg (Membrane purification of Cl_2 gas part I and part II in 2000, and Purification of chlorine gas with membranes in 2001). The objective of the project was to search for a possible membrane for industrial production of pure, dry chlorine gas. The process gas is concentrated in chlorine (up to 90% of Cl_2) and normally contaminated with O_2, N_2 and H_2. Nevertheless, in this study, only the permeation of Cl_2 and O_2 was studied. A membrane with high permselectivity for either O_2 or Cl_2 was considered to be a suitable membrane for the purification process. The four membrane types were polydimethylsiloxane (PDMS) membrane, perfluorinated membrane, pyrolyzed carbon molecular sieve membrane (CMS) and glass membrane. Hagg concluded that PDMS is the best solution for the purification of the process gas stream since it gave stable performance in the aspects of selectivity and permeability for a longer period of time. In the case of CMS, Cl_2 was completely retained but, unfortunately, the membrane was easily plugged by Cl_2 in the range of temperature studied (35-90°C) causing the permeation flux to lower as a function of time. To avoid the plugging of the CMS membrane, the author suggested the separation be performed at a temperature above 200°C or the membrane should be surface treated or modified.

Polymeric materials under many trademarks are sold commercially as protective coatings. The performances of the materials vary depending upon their chemical structures and the additives. Some of the materials sold in the market are shown in Table 2.3.

All of those manufacturers claim that their coating materials have good resistance to chlorine and other aggressive chemicals including hydrochloric acid. However, according to study at Centre for Nuclear Energy Research (CNER) in March 1999, breakthrough of chlorine was found in many trademarked materials. CNER tested ten different polymers and three metals as part of the development of a sensor to measure hydrogen concentration in the presence of moist chlorine at 80°C. The objective of the project was to search for a potential sheathing material for the sensor. The tested polymeric materials included Kynar®, Teflon®, Nafion®,

Saran®, Viton®, Nylon 4,6, Halar®, PVC, silicone rubber, and Derakane®. Tantalum, Hastelloy C and Palladium were three metals that were also tested. The H_2 and Cl_2 permeability coefficients at 80°C of all the materials and metals were determined. The ratio of the H_2 and Cl_2 permeability coefficients of the material was desired to be at least 10,000 for the potential candidate. The results showed that epoxy vinyl ester based Derakane® is the most promising material since it was the only polymeric material which did not allow chlorine breakthrough during a nine-day-period using a 0.75 mm thick sample.

Table 2.3 Examples of trademarked materials in the market.

	Tradename	Producer	Chemical name
1	Teflon	DuPont	Polytetrafluoroethylene
2	Saran	Dow Chemical Company	Polyvinylidene chloride (PVDC)
3	Kynar	Elf Atochem North America Inc.	Polyvinylidene fluoride (PVDF)
4	Viton*	DuPont Dow Elastomers	Fluoroelastomers (FKM)
5	Halar	Ausimont USA, Inc.	Copolymer of Ethulene and chlorotrifluoroethylene
6	Vipel*	AOC	Bisphenol A Epoxy Vinyl Ester or polyester and others*
7	CoREZYN*	Interplastic Corp.	Bisphenol A Epoxy Vinyl Ester or polyester and others*
8	Derakane*	Dow Chemical Company	Bisphenol A Epoxy Vinyl Ester or polyester and others*

* A full series of Viton®, Vipel®, CoREZYN® and Derakane® have not been shown in this table.

Studies of the search for a potential chlorine protective material for the sensor to measure hydrogen concentration in the presence of moist chlorine were carried out further by Kitjaroenvong in 2000 and Khamsa-Ang in 2001. From Kitjaroenvong's work, no chlorine was detected through 0.215-0.959 mm thick Derakane® coated on teflon samples for up to 36 hours of continuous contact with chlorine. Moreover, besides the Derakane® resin, Kitjaroenvong also tested other coating materials which were different from those which had been previously tested by CNER. She found another suitable material called Fluorodyn® Caulk (made with Viton®). The 0.254 and 0.347 mm thick Fluorodyn® Caulk gave no chlorine breakthrough in 69 and 42 hours, respectively. In addition, membrane made with Viton® showed a high permeation of hydrogen. Later in 2001, more experimental studies about epoxy

vinyl ester based Derakane® and fluoroelastomer Fluorodyn® materials were conducted by Khamsa-Ang. She found that a membrane having a 0.56 mm thick epoxy vinyl ester based Derakane® resin layer on a 0.15 mm Teflon® support can block chlorine up to 160 hours. For Fluorodyn® materials, it was reported that a 0.59 mm thick Fluorodyn® caulk and a 0.70 mm thick Fluorodyn® sheet gave chlorine breakthrough times of 39.25 and 15.00 hours, respectively.

2.4 The Development of a Device to Measure Hydrogen in The Presence of Moist Chlorine

The Centre for Nuclear Energy Research (CNER) has been attempting to develop a device to measure hydrogen in the presence of moist chlorine since March 1998. The first type of sensor studied was a Pd/H electrical resistance sensor (detailed picture shown in Figure 2.19). This type of sensor utilizes the dependency of the electrical resistance of palladium, upon the concentration of absorbed hydrogen in the metal. The ratio of the resistance of hydrogen-absorbed palladium to that of clean palladium at temperature T, is proportional to the hydrogen mole fraction in palladium; x_H as shown in Eq. (19).

$$\rho(x_H) = \frac{R(T, x_H)}{R(T, x_{H=0})} = 1 + kx_H \tag{19}$$

where k is a linear function of reciprocal absolute temperature.

Since palladium absorbs hydrogen dissociatively, the mole fraction of hydrogen in palladium relates to the partial pressure of hydrogen in the contacting gas; p_{H2} as described in Eq. (20).

$$K_{g,T} = \frac{x_H^2}{p_{H_2}} \tag{20}$$

$K_{g,T}$ is the equilibrium constant of the chemical reaction of hydrogen absorbed on palladium. Then, by combining Eq. (19) and (20), the relationship of the concentration of hydrogen in the gas stream and the electrical resistance of palladium can be written as stated in Eq. (21).

$$\rho(x_H) = 1 + k_g p_{H_2}^{1/2} \tag{21}$$

where $k_g = kK_{g,T}^{1/2}$

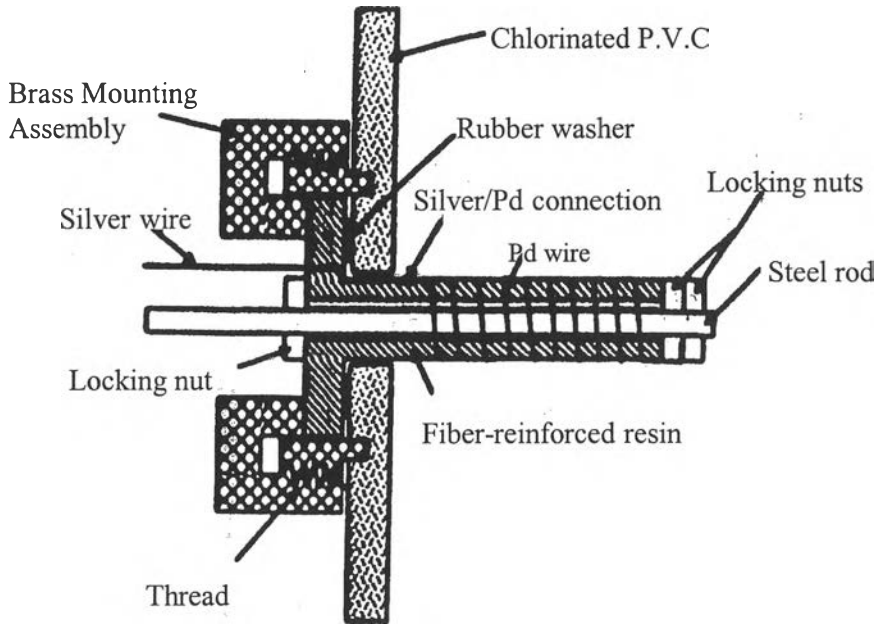

Figure 2.19 Cross section of the Pd/H electrical resistance sensor.

Palladium catalyzes the reaction between hydrogen and chlorine resulting in a change in the absorption of hydrogen by the palladium, which causes the sensor to give an erroneous result of the hydrogen concentration. Hence, the first phase of the project focused on the search for a sheathing material or a hydrogen-selective membrane that protects the metal from direct contact with Cl_2 (CNER, 1998). After Derakane® resin was identified as the most promising material in March 1999, the project then focused on optimizing the response time of the Derakane® sheathed sensor.

Later in January 2000, an electrochemical potentiometric sensor was also studied in the research project. Both types of sensors; Pd/H electrical resistance sensor and potentiometric sensor, with and without Derakane® coating, were tested. Both types of sensors showed slow responses to the change of hydrogen concentration in the $Cl_2/Air/H_2$ stream at 80°C. It was suspected that there was a permeation of chlorine through the Derakane® resin, which contrasted to the study in March 1999 that found no Cl_2 passed through Derakane® resin. Then, the Derakane® resin was re-tested for the ability to resist chlorine by Kitjaroenvong (2000). Other types of materials which had not been tested before were also studied. No chlorine was detected through a membrane made with Derakane® resin. Furthermore, another suitable material; Fluorodyn® Caulk, was proposed. CNER continued the investigation with a palladized Pd/H electrical resistance sensor (March 2000). It was found that the deposition of palladium crystals on Pd wire by an electrolytic process utilizing an aqueous solution of palladium chloride (palladizing process) could improve the response time of the sensor. Furthermore, the uncoated sensor gave much quicker response time than that of the Derakane®-coated sensor.

Later in May 2000, a theoretical prediction of the response time of Derakane® coated Pd wire was made. CNER suggested that, theoretically, it should be possible to reduce the response time to an acceptable value by changing the geometry of the probe. As can be seen in Figure 2.20, the response time can be improved by reducing the Pd wire diameter, the thickness of the coating or both.

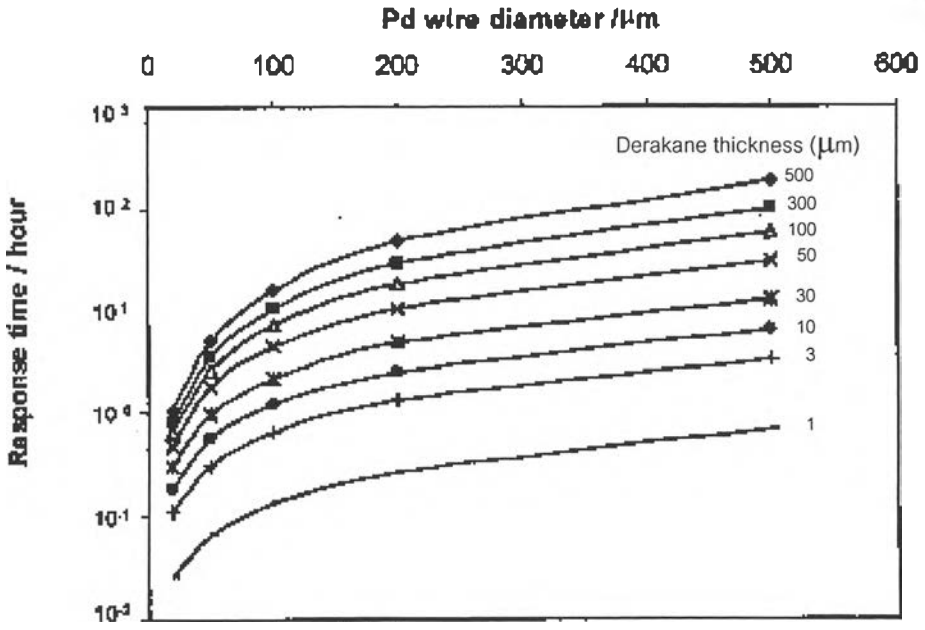

Figure 2.20 Response time of Derakane® coated Pd wire predicted by theoretical calculation (CNER, May 2000).

An electrochemical amperometric sensor (shown in Figure 2.21) was added into consideration in October 2000. Information obtained from this type of sensor depends on the linear current-concentration relationship governed by Faraday's law (Eq. 22).

$$J = \frac{I}{zFA} \tag{22}$$

where J is the flux of chemical species that reacts with the electrode in the sensor

I is the current measured from the external circuit

z is the number of electrons involved in electrochemical reaction

F is Faraday's constant

A is the area of electrode.

The reactions which occur at the electrodes are

Pt Anode: $H_{2(aq)} \rightarrow 2H^+ + 2e^-_{ca}$ (23)

External circuit: $2e^-_{an} \rightarrow 2e^-_{ca}$ (24)

Ag/AgCl Cathode: $2e^- + 2Ag_{(s)}^+ \rightarrow 2Ag_{(s)}$ (25)

Net Reaction: $H_{2(aq)} + 2Ag_{(s)}^+ \rightarrow 2H^+ + 2Ag_{(s)}$ (26)

The sensor requires periodic regeneration and/or recalibration since loss of Ag^+ occurs at the cathode. A protective material or hydrogen-selective membrane is also needed for this type of sensor. Thus, the flux of hydrogen available to react at the Pt electrode is equal to the flux of hydrogen permeating through the membrane. The current is then defined as in Eq. (27).

$$I = \frac{zFAP_{H_2}}{l} p_{H_2} \tag{27}$$

where P_{H2} is the permeability coefficient of the membrane

l is the thickness is the membrane

p_{H2} is the partial pressure of hydrogen in the gas stream.

Hence, when the current from the external circuit of the membrane sensor is measured, the concentration of H_2 in the feed gas stream is known.

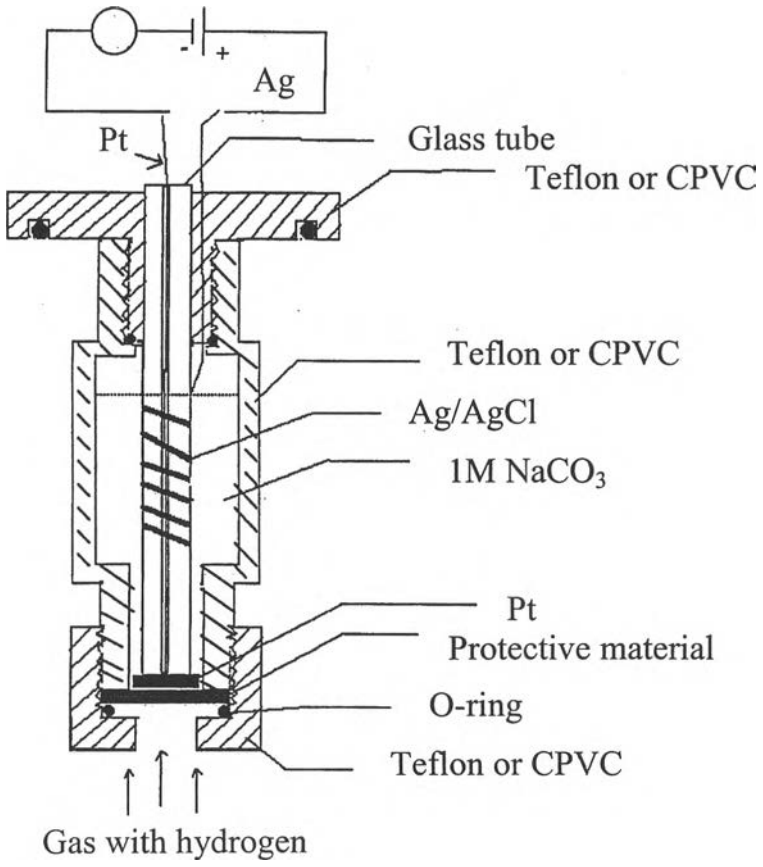

Figure 2.21 Electrochemical Amperometric sensor for Hydrogen

The study of the potentiometric sensor was stopped since the amperometric-typed sensor is universally reported to give more accuracy. Uncoated and coated amperometric sensors using Derakane® and another interesting coating material, Fluorodyn® Caulk, proposed by Kitjaroenvong (2000) were studied. The experimental results indicated that the sensor sheathed with either Derakane® or Viton® responded quickly to the change of hydrogen concentration in both reactive and non-reactive gas mixtures.

In the case of the Pd/H electrical resistance sensor, as found from previous studies, the unacceptably long response time of the coated sensor may overcome by reducing the amount of palladium and/or reducing the thickness of the coating material (Derakane® or Viton®). Thus, a sensor consisting of a Viton coating over a stainless steel tube on which Pd was electroplated was designed. The mathematical study indicated that the newly designed sensor should give a lower response time than the one developed earlier. Nevertheless, the response time of the amperometric sensor to a change of hydrogen concentration was a lot less than the calculated response time of the newly designed Pd/H electrical resistance sensor. The faster response of the amperometric sensor was noted to be because the hydrogen concentration measurement principle of the amperometric sensor does not depend on the absorption of hydrogen on the metal as in the electrical resistance sensor. This resulted in the research project focusing solely on the amperometric sensor. The periodic recalibration and/or regeneration of the platinum electrode, the design of the sensor body as well as the electrolytes used in the sensor are areas to be studied further.